FACTA UNIVERSITATIS
Series: **Working and Living Environmental Protection** Vol. 12, N^{o} 3, 2015, pp. 341 - 358

DYNAMIC RESPONSE OF HEAVY-LIFTING SHIPYARD MACHINES TO RESONANT ENVIRONMENTAL LOAD CONDITIONS

UDC 621.12:624.042.41

Goran Radoičić, Miomir Jovanović

Faculty of Mechanical Engineering,
Department of Transport Engineering and Logistics, University of Niš, Serbia

Abstract. *Climate changes on the planet have led to the appearance of extreme natural influences on large structures in ports and shipyards, as well as at-sea structures. One of the most variable meteorological effects in space and time is the wind. This paper provides the manner of dynamic modelling of wind loads on a tall portal-rotating crane structure. The gust of wind is modelled as a wave quantity variable in time and altitude of flow. Dynamic wind activity on tall structures is used to obtain structure's behaviour with regard to extreme climate events when frequently resonant influences occur. This is performed by non-linear transient FEM analysis. Structural damping is modelled by conversion to the equivalent viscous damping. Eigenfrequencies are obtained by applying the Lanczos method which combines the tracking method and the transformation method. The paper contains an originally developed dynamic model, experimentally verified stiffness, and internal static quantities. The aim of the paper (Case Study) is to obtain the wind activity which would cause the loss of dynamic stability of the crane due to multiple resonant gusts of wind. Such analyses can be employed to determine the real risk from a potential failure in tall structures caused by environmental, meteorologically registered activities.*

Key words: *wind load, dynamic response, shipyard cranes*

1. INTRODUCTION

The effect of strong wind (storm) on tall cranes can directly endanger their integrity and stability. A change in the crane mode represents a safety measure in such cases, i.e. a crane should stop operating and enter a safe rest position. These safety possibilities can be found in certain transport machinery structures, such as truck cranes and mobile working

Received November 13, 2015 / Accepted December 2, 2015
Corresponding author: Goran Radoičić
University of Niš, Faculty of Mechanical Engineering in Niš, 14 Aleksandra Medvedeva St, 18000 Niš, Serbia
E-mail: goran.radoicic@jkpmediana.rs

platforms. Apart from a significant influence of wind loads, large transport machines such as at-sea and off-shore structures are also subjected to the influence of ocean loads, temperature, sea depth, characteristics of the sea bottom, snow and ice. An example of a complex load exerted on an off-shore support structure is the loading of a jack-up platform, today highly exploited structure, [1], covered by the standard [2]. Such structures possess the survival mode which suspends all working operations in them in cases of extreme weather conditions. Unfortunately, certain crane classes do not have the option of switching to the safe mode due to their design and position (purpose). One such structure is the Shipyard portal-rotating Crane (SC) which is exposed to extreme collapse risks. Shipyard cranes are characterized by a tall structure and a large surface exposed to the variable wind influence. Furthermore, the geometry of a SC base is ten times smaller than its height. Wind gusts can cause galloping and resonant vibration and structural collapse. Several resonant collapses of cranes and other structures (bridges, towers, wind turbines, etc.) have occurred throughout the world recently, [3]. Even though extreme environmental loads appear only rarely (outstanding loads), they have to be taken into account when designing transport machines and other constantly exposed structures. New design criteria of these machines should allow for a more efficient structural response to extreme environmental loads (at the first sign of a load) through an optimal distribution of the stiffness of members, [4], [5].

1. RANDOM AND EXTREME WIND CHARACTER

As one of the most important meteorological phenomena, wind appears in the lowest layer of the atmosphere – the troposphere, most often as approximately horizontal turbulent air flow. Wind acts as a dynamic load on an observed structure, and it is stochastic in nature. The definition of wind, as a vector quantity, requires the knowledge of wind speed (magnitude) and direction (sense of direction). Wind observation (measurement of characteristics) is performed with an anemometer and an anemograph (ground winds), as well as radio probe systems, pilot balloons, Doppler radar, aircraft navigation systems and GPS dropwindsonde (high-altitude winds), [6], [7], [8]. Today, the majority of measurements of wind speed and direction are performed using modern GPS probes at altitudes of up to 5000 m and above, with the aim of creating a vertical profile of the wind above the ocean surface. To empirically calculate the wind force according to its characteristics, i.e. the form of manifestation towards the environment, several scales are used: Beaufort scale, Fujita scale, TORRO scale, Saffir-Simpson scale. An approximate determination of the wind speed at the altitude of H=10 m above the sea level according to the Beaufort scale (Francis Beaufort) is carried out using the empirical formula:

$$v = 0.836 \cdot Bf^{3/2} \quad [\text{m/s}] \tag{1}$$

where Bf = 0÷12 is the Beaufort number used to numerically represent wind strength and characteristics, [9].

Since it is the case of a random phenomenon, the average wind speed, depending on the altitude, can be represented rather well by a single number of probability distributions. These are most often: logarithmic, exponential, Weibull, Gumbel, etc. The vertical profile of wind speed is formed stochastically by applying one of the above distribution methods,

[6], [10-15], and on the basis of 50 or 100-years old statistical records on the measured wavelike air flow speeds (random values). Fig. 1 shows the vertical wind profile (speed and direction) obtained by experimental observation of Hurricane Rita (2005) using a GPS dropwindsonde, [6].

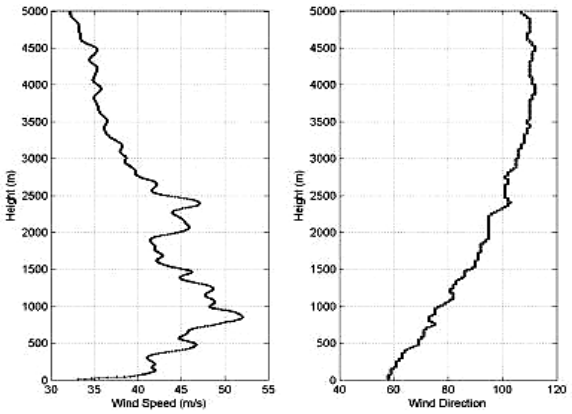

Fig. 1 Vertical wind profile, [6]

The first significant deadly hurricane, ranked as number three in strength out of all hurricanes (Category 5 according to the Saffir-Simpson Hurricane Wind Scale – SSHWS) in the history of the USA, was Hurricane Katrina (Fig. 2). Category 5 according to the SSHWS scale implies a wind speed of over 70 m/s (252 km/h). Hurricane Katrina lasted eight days, increasing in power in the period from August 23 to 30, 2005. To date, it is the most costly natural disaster in the USA. It killed 1245–1836 people in Louisiana (the majority of casualties), Florida, the Bahamas, and Cuba. The damage incurred amounted to $108 billion [16], and the surface area of 560 km^2 of land disappeared (turned into water surface). Katrina, Fig. 2, is of extreme importance since it represents a turning point in the understanding of large-scale hurricane danger and the protection of population and property from it.

Fig. 2 NASA satellite image of the Gulf of Mexico: Hurricane Katrina, August 28, 2005. Lowest atm. pressure: 902 mbar, highest wind speed: 280 km/h (in the duration of at least 1 min) measured at the altitude of 10.1 m from the ground, [17]

The ranking of extreme – hurricane winds according to the incurred damage and the assumed wind speed is performed in the USA by using the six-degree Fujita scale (F0÷F5). In Europe, the TORRO scale is often employed to rank hurricane winds according to their strength. Table 1 offers an overview of several most recent hurricanes in the Atlantic with their corresponding categories of strength according to SSHWS, where some of them possessed extreme speeds of almost 300 km/h (the fourth category). By the by, according to the available data, the highest wind speeds of 346 km/h were recorded in the Western Pacific during Typhoon Nancy in 1961.

It can be concluded, from the reports of the storm-monitoring bodies, that the number of hurricane casualties have dropped recently due to the application of modern technologies for monitoring, prediction and notification, as well as more efficient population evacuation. On the other hand, the value of the damage caused by storms has risen significantly as a result of building expansion along the coasts and in their vicinity. The case study analysis in the paper implies a Category 1 wind load according to SSHWS and the wind speed of 33–42 m/s.

Table 1 Hurricanes in the last several years, [18]

Hurricane (year)	Geographical area	Wind speed v [mph]	Category SSHWS
Edouard, 2014	The Eastern and Central Atlantic	120	3
Ingrid, 2013	Mexico	85	1
Humberto, 2013	The Eastern and Central Atlantic	90	1
Sandy, 2012	Caribbean and the East Coast-USA	115	3
Isaac, 2012	The Mexican Gulf Northern Coast	80	1
Igor, 2010	Bermuda and the Eastern Seaboard	155	4
Paloma, 2008	The Western Caribbean	145	4
Ike, 2008	Texas	145	4

The aerodynamic wind action on a crane structure is expressed in two planes, the horizontal and the vertical. The aerodynamic force that acts in the horizontal plane is perpendicular to the wind flow direction and caused by swirling during the flow of air around a body which does not have an aerodynamic shape (von Kármán vortices). On the other hand, the aerodynamic wind force, which acts in the vertical plane, is caused by the air flow of relative speed v_r and has the angle of incidence γ in relation to the normal of the exposed (vertical) machine surface. This force causes the so-called galloping effect, i.e. galloping oscillations of a structure. The aerodynamic force F_a^{v} in the vertical plane is broken down into two components: the drag force F_d in the direction of speed v_r and the lift force F_l perpendicular to this direction, [5]. Thus, the force F_a^{v} is a variable in time and it possesses a harmonic character and direction in this paper which corresponds to the angle of incidence $\gamma = 0°$.

2. MATHEMATICAL BASIS OF ENGINEERING DESIGN

To solve the forced vibrations of a discrete mechanical system of a portal-rotating crane in this research, the following differential equation of motion is used:

$$[M]^t\{\ddot{u}\} + {}^t[C]^t\{\dot{u}\} = {}^t\{f_{\mathrm{ext}}\} - {}^t\{f_{\mathrm{int}}\} \tag{2}$$

where: [M] and [C] are the matrices of mass and damping, $\{f_{ext}\}$ and $\{f_{int}\}$ are the external (excitation) and internal (elastic) forces of a set of finite elements, $\{\dot{u}\}$ and $\{\ddot{u}\}$ are the first (speed) and second (acceleration) time extractions of the structural displacement u, t (the left superscript) is the moment in time in which quantity is observed (i.e. acceleration, damping, speed and force).

Geometric nonlinear structural analysis requires the calculation of stress $\{\sigma\}$ in the current structural configuration, and the integration of those stresses in the current structural continuum ${}^{t}V$, with the aim of obtaining internal structural forces, therefore, it can be written as:

$$ {}^{t}\{f_{\text{int}}\} = \int_{{}^{t}V} {}^{t}[B]^{t}\{\sigma\} d\,{}^{t}V \tag{3} $$

where [B] is the matrix of deformation-displacement (defining the linear members of the deformation field) of the FE set.

The integration of dynamic equilibrium equation (2) is the most time-consuming part of the FEM transient computation. Geometrically nonlinear analysis requires direct integration methods, which are divided into a group of explicit methods and group of implicit methods. The main differences between them are the expense of calculating one time step, the time step size due to stability criteria and at which moment in time the equilibrium is considered.

The equilibrium (2) at time t is suitable for the time-marching-forward schemes of explicit methods. They are rather inexpensive regarding the computational effort required to compute a single time step. However, the size of the time step is restricted and has to be smaller than a certain critical value for the solution to be stable. The critical time step directly depends on the largest eigenfrequency of the finite element assemblage influenced by the discretization of the structure. Another consequence of a short time step is that the iteration errors due to nonlinearities are negligible, hence no iterations are performed.

The implicit methods are unconditionally stable, which accounts for their advantage. However, the time step is certainly limited by the required level of accuracy. More precisely, it depends on the highest eigenfrequency in the structural response that is of interest for the analysis. A general recommendation is to choose the time step size so as to split the period of the highest eigenfrequency of interest into 8–10 segments. It should also be taken into account that, within an implicitly integrated geometrically nonlinear transient analysis, large time steps imply a relatively large computational effort to resolve a time step due to the coupled system of equations and necessary iterations.

Finally, to resolve the structural configuration at time $t+\Delta t$, the equilibrium equation for the very same moment in time (i.e. $t+\Delta t$) is used.

The structure considered in the paper is made of steel and the conditional stability of an explicit time integration would impose a critical time step of the order of magnitude of $10^{-7} \div 10^{-5}$ s. Taking additionally into account the considered excitation and the range of structural vibration modes that is of interest, a reasonable choice would be an implicit time integration scheme with a time step of 10^{-3} s. Such a choice also filters out effectively higher modes in the structural response. The choice of the authors is the Newmark time integration. The system of equations for geometrically nonlinear structural dynamics for time $t+\Delta t$ reads:

$$ [M]\,{}^{t+\Delta t}\{\ddot{u}\}^{(k)} + {}^{t+\Delta t}[C]\,{}^{t+\Delta t}\{\dot{u}\}^{(k)} + {}^{t+\Delta t}[K_T]\,{}^{t+\Delta t}\{\Delta u\}^{(k)} = {}^{t+\Delta t}\{f_{\text{ext}}\} - {}^{t+\Delta t}\{f_{\text{int}}\}^{(k-1)} \tag{4} $$

where $[K_T]$ is the tangential stiffness matrix, Δ denotes the increment of a quantity and k denotes the iteration. The tangential stiffness matrix together with the increment of displacements enables estimation of the internal forces at time $t+\Delta t$. According to the updated Lagrangian formulation, the tangential stiffness matrix is computed as:

$$ {}^{t}[K_T] = {}^{t}[K_L] + {}^{t}[K_\sigma] \tag{5} $$

where ${}^{t}[K_L]$ is the linear stiffness matrix and ${}^{t}[K_\sigma]$ is the geometric stiffness matrix, both determined for the current structural configuration, i.e. at time t as:

$$ {}^{t}[K_L] = \int_{{}^{t}V} {}^{t}[B]^{\mathrm{T}} [H] {}^{t}[B] \; d\,{}^{t}V \tag{6} $$

$$ {}^{t}[K_\sigma] = \int_{{}^{t}V} {}^{t}[B_{NL}]^{\mathrm{T}} \; {}^{t}[\sigma] \; {}^{t}[B_{NL}] \; d\,{}^{t}V \tag{7} $$

where $[H]$ is the Hooke's matrix, $[B_{NL}]$ is the matrix that yields the nonlinear part of the strains and $[\sigma]$ is the stress state given in matrix form, all of them defined at the current structural configuration, i.e. at time t.

3. STRUCTURAL MODEL DEVELOPMENT

The testing of the dynamic performance of a shipyard crane was performed by simulation on a numerical model which accurately represents the real existing structure. The FEM crane model from the previous research [19] has been enhanced and it now contains 221 finite element and 144 nodes with 864 degrees of freedom. The modelling of the complex FE model from Fig. 3 employed the beam-tip, plate-tip and spring-tip finite elements. Portal shipyard cranes have a slightly higher coefficient of the total structural damping G since it is the case of heavier structures in relation to the frame structures of tower cranes. Based on the experimental research of frame structures [20] and [21], and for the purpose of transient analysis of a shipyard crane, the authors adopted the safe coefficients of structural damping (for these classes of metal structures and great heights of cranes) in the value of G=0.05÷0.06. Nonlinear static, modal and transient FE analyses of the structure were performed using the MSC NASTRAN software.

The experimental verification of the developed model stiffness was carried out on a crane from the Uljanik shipyard in Pula (Republic of Croatia), [22]. The crane's features are: the support structure of maximally 67 m in height and the maximal range of 40 m, 6×8 m portal base, the total mass of 400 t, and the level-luffing system in the form of a four-bar mechanism with its members and rocker connected by joints. The crane capacity is 25/15/5 t at the range of 27/37/40 m, respectively. The crane mechanisms are positioned on a mast of 30 m in height, above which, on a compact rotating platform, a tower is mounted (truss structure). The tower contains the basic elements for level luffing: rod, jib and rocker (Fig. 3). The level-luffing drive mechanism contains a spindle which acts on the basic jib. The jib system is balanced by using a structure in the form of a four-bar mechanism – an arm and a balancer with a counter-weight of 21 t in mass. The balancing of the entire rotating structure of the crane is done using a 100 t weight, located on the rotating platform.

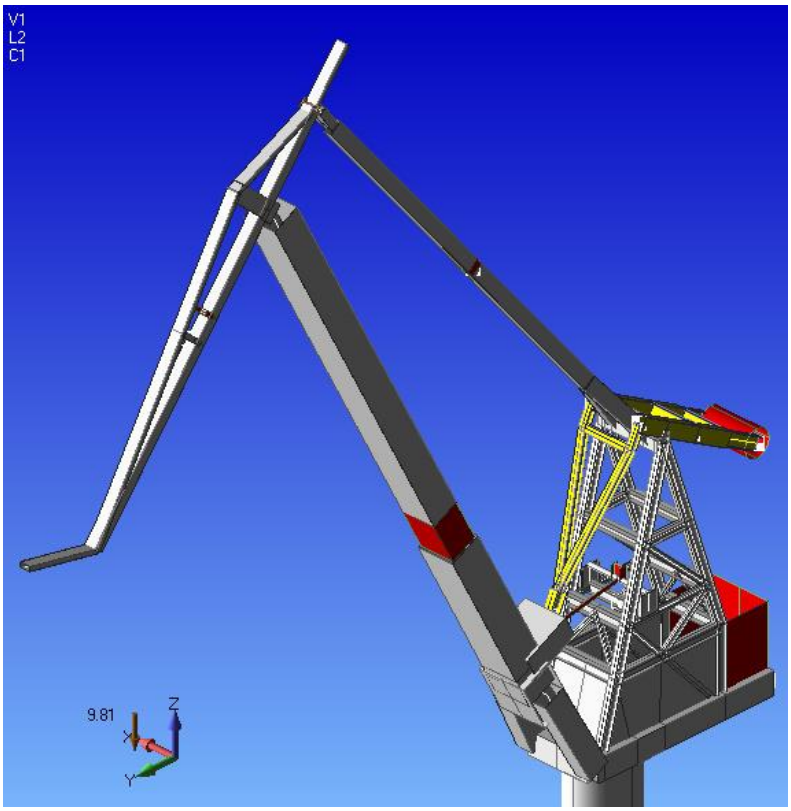

Fig. 3 FE model of the portal-rotating crane

The quality of modelling (distribution and characteristics of introduced finite elements) was checked by verifying the elastic properties of the top of the support structure. The rocker top path was experimentally determined by the geodetic levelling method (optical method). Measurement results are shown in Fig. 4, which incorporates analytical, numerical and experimental results. Experimental results are given by dotted square symbols for operations under loads. Numerical results of the rocker top elastic line, obtained by FE analysis, are presented with a black curve. The other, light green continuous curve shows the initial positions of the rocker top path (the theoretical trajectory of the stiff mechanical model). Deflection deviation from numerical and experimental research (model control) amounts to maximally 10.2 % in the entire level-luffing range, [22]. Deviations are mainly nonlinear in nature and conditioned by an error in the manufacturing of large members of the metal structure of the crane and the rheological changes in the geometry of the track on the sea shore.

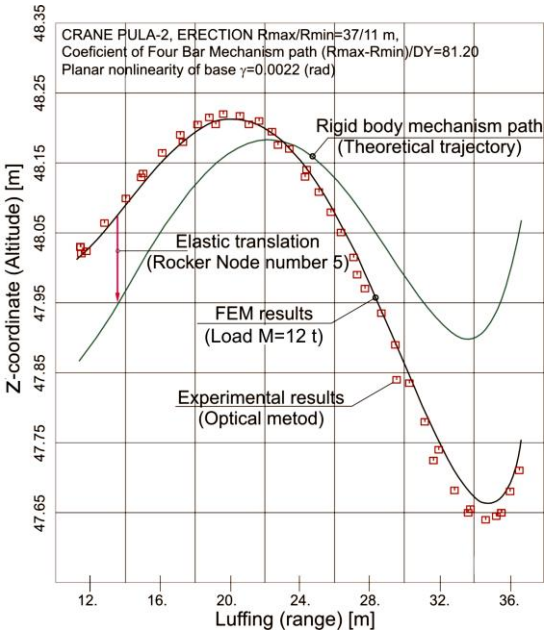

Fig. 4 Diagram of a comparison between experimental and theoretical elastic characteristics (verification), [19]

4. WIND LOAD MODELLING

For the analysis of the effect of extreme winds on the structure of a tall transport machine, the authors chose a portal-rotating crane located in a shipyard and constantly subjected to air influences (without the possibility of shifting into a safe position). The crane observed as a multi-body comprising several sub-structures, for example: portal, mast, platform, operator cabin, counterweight, pylon, jib, rod, level-luffing mechanism, and rocker. The majority of these can be represented using frame-type models and beam-type elements. The above types of elements can be considered sufficiently aerodynamic so as to approximately neglect the influence of the aerodynamic force due to swirling, thus it will not be taken into account in transient analysis. Only the aerodynamic force F_a^{ν} will be considered as a time-variable internal harmonic load caused by wind gusts in the vertical plane.

In this case study, the distorting force of the wind will be observed in two ways:

A. As a static load with the aim of defining the boundary conditions of static stability,
B. As a gust of wind in the sense of a dynamic load modelled by a harmonic function with the aim of defining the dynamic reserve of the structure.

Since the crane is 67 m tall, the influence of the wind is observed in various heights from the ground discretely in the gravity centres of the elementary exposed surfaces of the structure. The exposed surface of the entire structure is divided into seven elementary surfaces A_i, $i = 1 \div 7$ (Fig. 5) in the direct calculation, with the same angle of incidence of the wind force $\gamma = 0°$ (perpendicular to the surface). When dimensioning the support

structure, the force of wind pressure on the structural members is considered steady load. Table 2 provides the values of gravity centres heights z_i (wind force points of incidence) of elementary exposed surfaces A_i with the description of the shape of the corresponding structural members, as well as the values of adopted aerodynamic shape coefficients C_s.

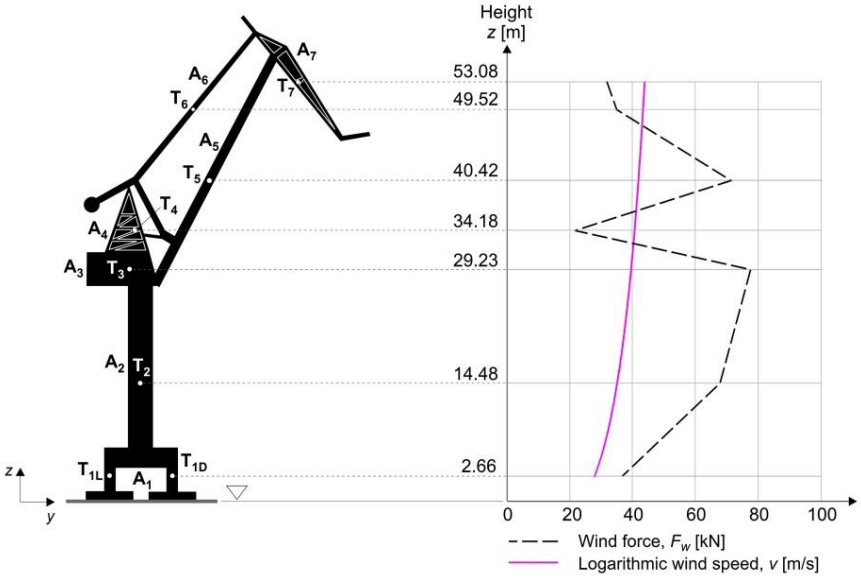

Fig. 5 SC model with elementary surfaces, wind speed (11) and wind force (8) depending on the height of surface gravity centres ***z***

The steady state of the wind effect on the structural components *i*, i.e. the elementary exposed surfaces A_i, is represented by the wind force $F_w(i)$, according to [2], [23]:

$$F_w(i) = \frac{1}{2}\rho_a C_s(i) A_i v^2(z) \cos\gamma \quad [\mathrm{N}] \tag{8}$$

where: ρ_a=1.225 kg/m^3 – the air density for dry air at the temperature of 15°C; C_s – the shape coefficient (taken according to the until recently valid standard SRPS U.C7.113); A_i [m^2] – the exposed surface of the each observed structural element (elementary surface at height z_i); v=$U(z)$ [m/s] – the wind speed at each observed height z, taking into account the geographic terrain roughness z_0; γ=0° – the angle between the direction of the wind effect and the normal to the surface of the observed element of the structure (if the wind acts perpendicularly on the surface then γ=0°, $\Rightarrow$ cos γ=1).

To calculate the vertical wind profile at a given height ***z***, two methods are used here. The first is the logarithmic profile method and the second is the power law method, [24], in the conditions of a 10-minute speed averaging $U(H)$ (reference speed) at a reference height of H=10 m.

The logarithmic wind speed profile is defined as:

$$U(z) = U(H)\left(1 + \frac{1}{k_a}\sqrt{\kappa}\,\ln\frac{z}{H}\right) \tag{9}$$

where: $U(z)$ – the current wind speed at the height z; $U(H)$ – the averaged wind speed at the reference height H=10 m at the exposure of T=10 min; H=10 m – the reference height; k_a=0.4 – the von Kármán constant; z_0=0.001-0.01 m, adopted z_0=0.01 m – the terrain roughness parameter for coastal areas with onshore wind (based on Panofsky and Dutton 1984, Simiu and Scanlan 1978, Dyrbye and Hansen 1997, [24]); z – the height of the observed point of incidence upon which the wind force acts; κ – the surface friction coefficient which is determined according to the relation:

$$\kappa = \frac{k_a^2}{\left(\ln\frac{H}{z_0}\right)^2} = \frac{0.4^2}{\left(\ln\frac{10}{0.01}\right)^2} = 0.00335 \tag{10}$$

The reference (basic) wind speed is adopted from the Overview of temporary and approximate reference wind speeds in the former SFRY with a return period of 50 years, [25]: $U(H) = v_{ref}$ (Pula) = 35 m/s. Thus the expression is obtained for determining the logarithmic wind speed profile at the height z:

$$U(z) = 35\cdot\left(1 + \frac{1}{0.4}\sqrt{0.00335}\,\ln\frac{z}{10}\right) \tag{11}$$

The alternative method to the logarithmic one is the power law method, [24], i.e.:

$$U(z) = U(H)\left(\frac{z}{H}\right)^{\alpha} = 35\left(\frac{z}{10}\right)^{\alpha} \tag{12}$$

where α is the power-law exponent which includes the terrain roughness effect z_0 and the reference height H=10 m, as follows:

$$\alpha = \ln\left(\frac{\ln\frac{z}{z_0}}{\ln\frac{H}{z_0}}\right) \Big/ \left(\ln\frac{z}{H}\right) \tag{13}$$

Substituting the quantities z, z_0 and H with numerical values in (13) yields the values of α (Table 2).

Table 2 Elements for calculating the force of wind pressure F_w

i	Exposed surface A_i [m^2]	Height z_i [m]	Element shape (for each of A_i)	Shape coefficient C_s [-]	Exponent α [-]
1	37.94	2.66	Rectangular cross section (beam)	2.0	0.16072
2	67.86	14.48	Circular cross section (cylinder)	1.2	0.14102
3	38.80	29.23	Steel plate	2.0	0.13457
4	12.94	34.18	Truss structure	1.6	0.13324
5	32.82	40.42	Rectangular cross section (beam)	2.0	0.13184
6	15.30	49.52	Rectangular cross section (beam)	2.0	0.13021
7	13.73	53.08	Truss structure	2.0	0.12966

Table 3 provides the values of wind speed depending on the height of gravity centres z_i of elementary exposed surfaces of the crane A_i, according to (11) and (12), and the discrete values of the force of wind pressure acting perpendicularly on the structure on each exposed surface A_i, according to (8). The expression for the force F_{wi} (8) contains the speed values according to the logarithmic profile, which will be used in further analysis bearing in mind that these speeds differ from the speeds calculated in line with the exponential profile only in their third decimal digit.

Table 3 Calculated wind speed and force for heights ***z*** of gravity centres for exposed surfaces

i	Height z_i [m]	Wind speed (log) $U(z)=v_i$ [m/s]	Wind speed (power) $U(z)=v_i$ [m/s]	Wind force (log) F_{wi} [N]
1	2.66	28.2934	28.2903	37205.16
2	14.48	36.8748	36.8756	67820.31
3	29.23	40.4322	40.4347	77700.12
4	34.18	41.2245	41.2273	21551.15
5	40.42	42.0737	42.0769	71169.81
6	49.52	43.1020	43.1058	34819.54
7	53.08	43.4536	43.4575	31758.40

After designing, the obtained technical solution of the tall crane was subjected to real dynamic analysis which does not operate with assumed dynamic coefficients of static force enlargement. On the basis of multiyear meteorological records, the real nature of the wind in the observed region was introduced in the function of time. Such analyses are closer to the actual development of the situation (recurrence) in the given off-shore locations and they represent a safer guarantee for the crane owner to preserve its stability. Wind gusts are wavelike in nature and they change in the function of time. The nature of wind influence has a random character, yet it may express a certain recurrence conditioned by seasonal cycles of nature and the environmental effects of the coast, such as the terrain directing the flow. That is why general models of transitional dynamic processes are used to analyse structure responses to the influence of the wind – transient analysis. Furthermore, excitations are taken in accordance with the meteorological documents for the observed previous period.

To determine the dynamic behaviour of the tall crane under the influence of the wind, the authors introduced a wave excitation caused by the most adverse harmonic effect of a single or more short and strong wind gusts. This sudden dynamic character of the wind effect can mathematically be expressed with a single or more harmonics so that the time

excitation function is a synchronous function of individual forces F_h (t) at certain parts of the structure, or:

$$F_h(t) = F_w \cdot f_w(t) = \frac{1}{2}\rho C_s A v^2 f_w(t)\cos\gamma \tag{14}$$

where: F_w – the steady wind force as a static effect, $f_w(t)$ – the harmonic function of the wind excitation.

Since the entire exposed surface of the crane, in the observed example, is divided into 7 elementary parts (i=1÷7), one can define a synchronous harmonic equation of discrete excitation according to (14) for each of the elementary surfaces A_i.

To observe the behaviour of the structure caused by the wind, the function of influence has to be expanded by the initial calm state due to the lack of the wind and the function of the calm state after the wind has passed. Such a function then comprises more parts. In the observed cases, the function of wind excitation $f_w(t)$ is formed from three chronologically connected (continuous) functions $f_n(t)$, n=1÷3, (15), (16).

$$f_w(t)_{1H} = \begin{cases} f_1(t) = 0, \quad t = 0 \div t_1, \quad (t_1 = 30\,\text{s}) \\ f_2(t) = \dfrac{1}{2} + \dfrac{1}{2}\sin\omega t, \quad t = t_1 \div t_2, \quad (t_2 = 33.18\,\text{s}) \\ f_3(t) = 0, \quad t = t_2 \div t_3, \quad (t_3 = 80\,\text{s}) \end{cases} \tag{15}$$

$$f_w(t)_{4H} = \begin{cases} f_1(t) = 0, \quad t = 0 \div t_1, \quad (t_1 = 30\,\text{s}) \\ f_2(t) = \dfrac{1}{2} + \dfrac{1}{2}\sin\omega t, \quad t = t_1 \div t_2, \quad (t_2 = 42.72\,\text{s}) \\ f_3(t) = 0, \quad t = t_2 \div t_3, \quad (t_3 = 80\,\text{s}) \end{cases} \tag{16}$$

In both cases, after a time of 30 s of the calm state (without wind) i.e. after the linear function $f_1(t)$, a gust of wind was simulated with one (15) and more (16) equal gusts with the same critical load period T_1=3.18 s (Fig. 6). For a closer definition of the unpredictable occurrence of the hurricane wind, the authors observed the natural dynamic effects with resonant structural properties from the failure events such as *Falcon Crane Liverpool* (39 m in height) which collapsed following a gust of 82 km/h wind which lasted for 1 sec, [3]. In this case study, the critical gust period is the lowest eigenfrequency of the structure oscillation period in the observed direction of the typical wind movement. This causes the resonant mode of structural oscillation. The modal analysis was used to determine this critical period (for the observed crane) which corresponds to the lowest crane eigenfrequency of $\omega_1=\omega_{min}$=0.3146 Hz. Several next frequencies which characterize the modal shapes of the support structure in the wind direction are given in Table 4.

Table 4 Some modal frequencies (in the wind direction)

Mode, i	Eigenfrequency, ω_i [Hz]	Mode, i	Eigenfrequency, ω_i [Hz]
1	0.3146	12	4.4299
3	0.7334	21	11.5832
5	1.6194	29	16.8452
11	4.2437	32	25.4837

In the simulation time segment $t_1 \div t_2$ the excitation function $f_w(t)$ has a harmonic (sine) shape $f_2(t)$, with one (1H, Fig. 6, left) and four (4H, Fig. 6, right) wind gusts (H – harmonic), while the other segments of the function (for the other segments of simulation time) are linear in shape. The excitation ends with a linear damping function $f_3(t)$, for the period $t_2 \div t_3$ (until the end of the simulation), which allows enough time to obtain extreme responses after the swaying random effect of the wind. The total simulation time in this case is 80 s.

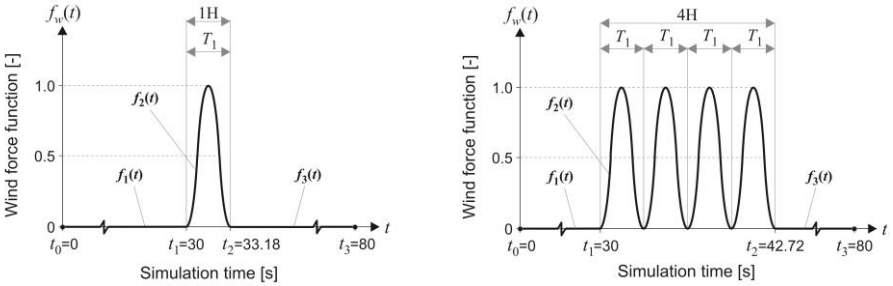

Fig. 6 Wind load (gust) harmonic functions: 1H (left) and 4H (right)

By selecting such a model of analysis, i.e. two harmonic wind functions with the same critical load period and different duration (1H and 4H), the authors emphasize the importance of the recurring load influence of the wind, i.e. the increasing number of gusts (sine function harmonics) on the dynamic response of the structure. The effect is reflected in the significant increase in the horizontal displacement of the tall structural members (rocker) and the dramatic rise in the reaction forces in the supports which are used to monitor the dynamic stability of the crane. If the selected extreme environmental random resonant effect of the wind is acceptable, then the portal has to be redesigned. Such an analysis belongs to the case study category and it is very logical when the off-shore environment is well-known.

5. Analysis of Extreme Influence Results

Elastic ground support elements (marked with E-59, E-60, E-70, E-71) remain compressed during the continuous static effect of the wind (reaction force is negative), which leads to the conclusion that the static response of the crane implies the sufficient stability of the structure. Moreover, the redistribution of internal forces within the portal legs (E-212÷E-215) occurs only in the pressure zone under the influence of the static wind load (the beam axial force is negative).

On the other hand, the dynamic response of the structure to the wind force effect of the magnitude F_{wi}, whose excitation function is represented by expressions (15) and (16), is presented through the results of the performed transient dynamic analysis. The parameters for numerical realization are: integration step 0.03 s and the number of steps 2667 (output sets). The periodic character of the wind is modelled using the lowest eigenfrequency of the crane as the most adverse possible case of loading (scenario). The resonant oscillatory mode with the critical wind gust period of T=3.18 s, which corresponds to the lowest eigenfrequency

of the structure, implies the pronounced dynamics (of displacement) of the upper section of the crane at the altitudes of above 40 m. Of particular interest is the rocker element whose top oscillates at extremely large amplitudes (-4.91÷4.47 m!) in the direction of the wind at the 4H load function. Horizontal displacement (in the static analysis) and horizontal oscillations of the rocker top (node N-38) in the direction of the wind, under the influence of the selected loads 1H and 4H, are shown in Fig. 7.

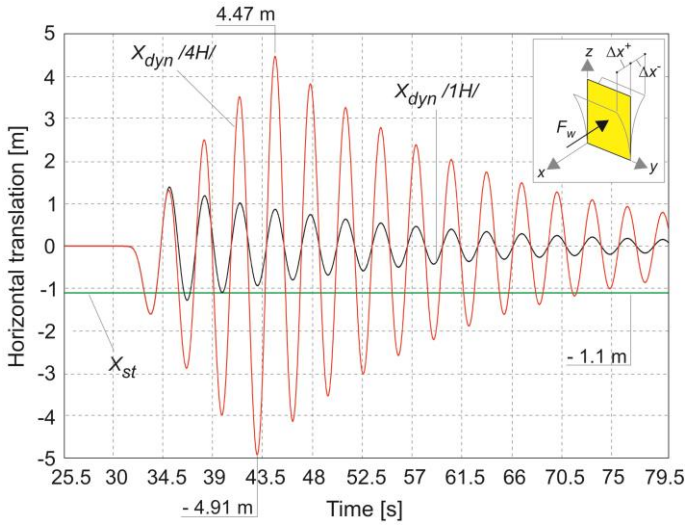

Fig. 7 Static and dynamic *x*-translation of Node 38 (The green straight line shows the displacement of the rocker top subjected to the statically treated wind)

Such a powerful internal excitation caused by a multiple harmonic function of the hurricane wind (4H, Fig. 6) leads to large horizontal oscillations (displacement) of the upper sections of the structure, which in turn results in the change in the reaction force sign in certain elastic supports, therefore instigating the separation of the structure from the ground.

The characteristic change in the elastic force sign occurs in support E-71 at the front side of the portal (exposed to the wind) (Fig. 8) and it causes a short-term dynamic instability of the structure, which manifests itself in the lifting of the base portal wheels. It is evident from Fig. 8 that the harmonic wind excitation 4H, through its gusts and period of gust of T=3.18 s, causes a constant increase in amplitudes, which tends to continue with the rising number of gusts. Realistically speaking, during a period of 30–50 years of the exploitation of a large shipyard crane, one can expect that an extreme event with such an unbelievable scenario will most probably occur.

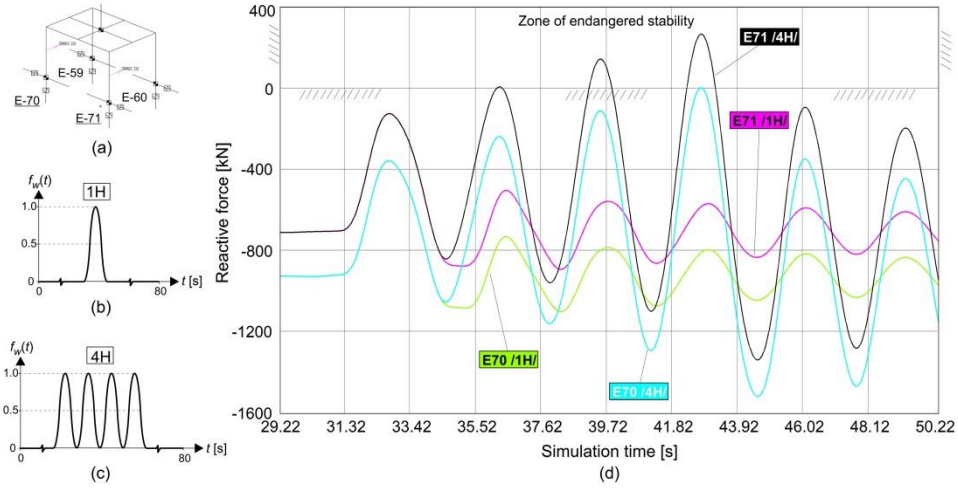

Fig. 8 (a) Positions of elastic supports E, (b) Wind load function with one harmonic – 1H, (c) Wind load function with four harmonics – 4H, (d) Reactive forces in elastic supports E-70 and E-71

Figure 9 shows the changes in internal force within the lower sections of the structure, which are subjected to the total static and dynamic load. The magnitudes of these forces are in the range characteristic of heavy tall structures. The damping of tall masses can be performed to a certain extent by enlarging the portal base and the general mass of the lower sections of the structure. This procedure can only be followed by active damping measures which are already being implemented in long-span suspension bridges.

The dynamic coefficient K_D (Table 5) can be formulated as a relation between internal forces $F_{A(h)}$, in the elements subjected to dynamic wind loads, and the steady effect of the wind F_A (static force) on the structure (17). However, if the design is checked in line with the maximal static wind force (oscillation-free continuous effect), the oscillation of tall crane masses will be excluded. The increase in dynamic forces, given in Table 5, is far larger due to the effect of tall mass oscillation than the other dynamic processes described using dynamic coefficients.

$$K_D = \frac{F_{A(h)}}{F_A} \tag{17}$$

Table 5 Axial forces F_A and dynamic coefficients K_D

Element	F_A* [N]	$F_{A(h)}$** [N]	K_D
E-212	-960863	-2110270	2.196
E-213	-689637	-1811226	2.626
E-214	-689961	-1406792	2.039
E-215	-961181	-1698516	1.767

* Internal static axial force in the finite elements of crane legs E-212 to E-215 (without wind load – only own mass of the crane);

** Internal dynamic (transient) axial force in the same elements (under wind load – sine function 4H). They have been taken as the highest magnitudes of forces, i.e. minimum (pressure) axial forces.

Observing Table 5, we can conclude that the dynamic coefficients for all observed elements have expressed and expected magnitudes as the consequence of the resonant wind load 4H.

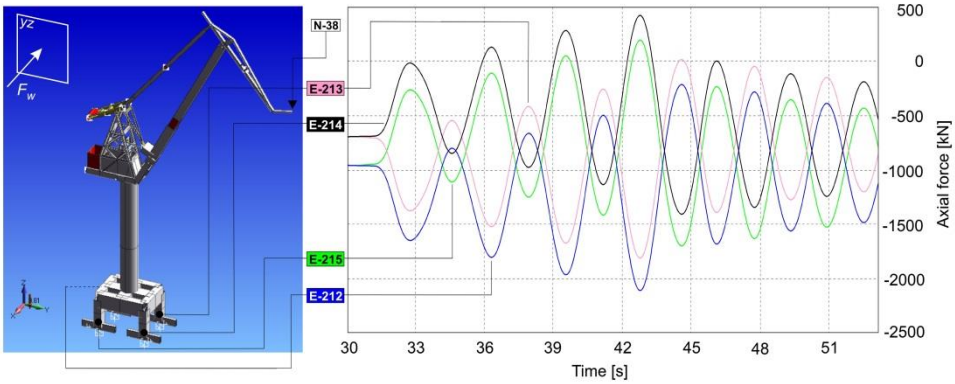

Fig. 9 Axial forces in crane portal legs (elements E: 212÷215)

6. CONCLUSION

A. A design adapted to the adverse environmental conditions is, in fact, the final category of design which sets the boundaries of the highest-level dynamic stability.
B. The best design implies the development of an original model of wind load in the observed environment, i.e. the working area of a machine. Such a model should define the real distribution of speeds and direction of air flow in the selected locality within the observed 50-year period.
C. Better adjustment of height, shape and basic position in tall cranes is possible by analyzing several case studies of wind effects. In this example, the portal base of the examined crane is not designed adequately for the most adverse direction of the extreme wind and it requires an increase in the span of portal rails.
D. Bearing in mind that case studies are based on the prediction of the internal influence shape and character, it would be logical to perform these analyses using stochastic calculations to assess the possibility of extreme influences. Since it is the case of random quantities, it is necessary to define the probable presence of extreme influences during the entire working life of structures.
E. New experiences with the wind demand from the structure design to acknowledge aerodynamic phenomena and introduce minimal swirling behind the surfaces around which the air flows. This would reduce the effect exerted upon the structure.
F. Furthermore, one has to seriously review the standards which regulate the statistically largest numbers of incidents. Case studies can also be conducted for operating cranes, which would lead to a better insight into real risks.
G. The most adverse responses of a tall structure are caused by a coincidence of the natural effects with the resonant property of the structure (in this case it was the lowest period of structural oscillation: T_1=3.18 s). If a load with the assumed magnitude and frequency (the resonant case) were to appear, a structure with the above design would not maintain its stability!

Acknowledgements: *This paper is part of the project TR-35049 implemented at the University of Niš, Faculty of Mechanical Engineering, and supported by the Ministry of Education, Science and Technological Development of the Republic of Serbia.*

REFERENCES

1. G. Rama, "An Automatized In-Place Analysis of a Heavy Lift Jack-up Vessel under Survival Conditions," Facta Universitatis – Series: Mech. Eng., Vol. 12(2), pp. 107-121, (2014).
2. Standard: Det Norske Veritas, DNV-RP-C104, November 2012.
3. N. Ristić, "Hazard Wind Influence and Collapse Structure," Nauka i praksa, GAF Niš, pp. 178-181, (2009).
4. N. Hajdin, Đ. Zloković, M. Vukobratović and V. Đorđević, "Active Structures," Proceedings of the Conference on Mechanics, Material and Constructions, Vol. 83, Book 2, Serbian Academy of Sciences and Arts, Beograd (Serbia), pp. 419-434.
5. S. Bošnjak, N. Zrnić and B. Dragović, "Dynamic Response of Mobile Elevating Work Platform under Wind Excitation," Strojniški vestnik – Journal of Mech. Eng., Vol. 55(2), pp. 104-113, (2009).
6. I.M. Giammanco, J.L. Schroeder and M.D. Powell, "Observed Characteristics of Tropical Cyclone Vertical Wind Profiles," Wind and Structures, Vol.15(1), pp. 65-86, (2012).
7. F.T. Lombardo, D.A. Smith, J.L. Schroeder and K.C. Mehta, "Thunderstorm Characteristics of Importance to Wind Engineering," Journal of Wind Eng. and Industrial Aerodynamics, Vol. 125, pp. 121-132, (2014).
8. C.D. Karstens, W.A. Gallus, B.D. Lee and C.A. Finley, "Analysis of Tornado-Induced Tree Fall Using Aerial Photography from the Joplin, Missouri, and Tuscaloosa–Birmingham, Alabama, Tornadoes of 2011," Journal of Applied Meteorology and Climatology, Vol. 52, pp. 1049-1068, (2013).
9. T. Fujita, "Proposed Characterization of Tornadoes and Hurricanes by Area and Intensity," Satellite & Mesometeorology Research Project, Research paper No. 91, University of Chicago (USA), (1971).
10. Y.J. Lu, Y-N. Chen, P-L. Tan and Y. Bai, "Prediction of Most Probable Extreme Values for Jackup Dynamic Analysis," Marine Structures, Vol. 15, pp. 15-34, (2002).
11. E.C. Morgan, M. Lackner, R.M. Vogel and L.G. Baise, "Probability Distributions for Offshore Wind Speeds, " Energy Conversion and Management, Vol. 52, pp. 15-26, (2011).
12. R. Chiodi, F. Ricciardelli, "Three Issues Concerning the Statistics of Mean and Extreme Wind Speeds," Journal of Wind Eng. and Industrial Aerodynamics, Vol. 125, pp. 156–167, (2014).
13. P. Sypka and R. Starzak, "Simplified, Empirical Model of Wind Speed Profile under Canopy of Istebna Spruce Stand in Mountain Valley," Agricultural and Forest Meteorology, Vol. 171-172, pp. 220-233, (2013).
14. X. Qin, J-S. Zhang and X-D. Yan, "Two Improved Mixture Weibull Models for the Analysis of Wind Speed Data," Journal of Applied Meteorology and Climatology, Vol. 51, pp. 1321-1332, (2012).
15. S-E. Gryning, E. Batchvarova and R. Floors, "A Study on the Effect of Nudging on Long-Term Boundary Layer Profiles of Wind and Weibull Distribution Parameters in a Rural Coastal Area," Journal of Applied Meteorology and Climatology, Vol. 52, pp. 1201-1207, (2013).
16. E.S. Blake, C.W. Landsea and E.J. Gibney, "The Deadliest, Costliest, and Most Intense United States Tropical Cyclones from 1851 to 2010 (And Other Frequently Requested Hurricane Facts)," NOAA Technical Memorandum NWS NHC-6, NHC Miami, National Weather Service, National Hurricane Center, Miami, Florida (USA), August 2011.
17. https://en.wikipedia.org/wiki/Hurricane_Katrina#/media/File:Katrina_2005_track.png
18. http://www.hurricaneville.com/historic.html
19. M. Jovanović, G. Radoičić and P. Milić, "Dynamic Sensitivity Research of Portal-Rotating Cranes," Proceedings of XIX International Conference on Material Handling, Constructions and Logistics, Belgrade (Serbia), 15-16 October 2009, pp. 61-66, (2009).
20. G. Radoičić and M. Jovanović, "Experimental Identification of Overall Structural Damping of System," Strojniški vestnik – Journal of Mech. Eng., Vol. 59(4), pp. 260-268, (2013).
21. M. Jovanović, G. Radoičić, G. Petrović and D. Marković, "Dynamical Models Quality of Truss Supporting Structures," Facta Universitatis – Series: Mech. Eng., Vol. 9(2), pp. 137-148, (2011).
22. M. Jovanović, "Supporting Structure Level Luffing System and Driving Mechanisms Resistance of Portal-Jib Cranes Optimization," Doctor's work, Faculty of Mechanical Engineering, University of Niš, 1990.
23. Standard: EN 1991-1-4-2005 +A1-2010
24. Standard: Det Norske Veritas, DNV-RP-205, October 2005.
25. O. Popović, M. Bogner, A. Simonović and S.Stupar, "O dimnjacima," ETA, Beograd (Serbia), (2011).

DINAMIČKI ODGOVOR TEŠKIH BRODOGRADILIŠNIH MAŠINA NA PRIRODNA REZONANTNA OPTEREĆENJA

Klimatske promene na planeti donele su pojavu ekstremnih prirodnih delovanja na velike objekte u lukama i brodogradilištima kao i na objekte na otvorenom moru. Jedan od najpromenljivijih meteoroloških uticaja u prostoru i vremenu je vetar. U ovom radu je pokazan način dinamičkog modeliranja opterećenja vetrom jedne visoke strukture portalno-obrtne dizalice. Nalet vetra je modeliran kao talasna veličina promenljiva sa vremenom i visinom (altitudom) strujanja. Dinamičko delovanje vetra na visoke strukture je korišćeno za nalaženje ponašanja strukture na ekstremne klimatske događaje kada se pojavljuju frekventno rezonantni uticaji. Realizacija je izvedena nelinearnom tranzijentnom FEM analizom. Strukturno prigušenje je modelirano konvertovanjem u ekvivalentno viskozno prigušenje. Nalaženje sopstvenih vrednosti izvedeno je Lanczos-ovom metodom koja kombinuje tracking metodu i metodu transformacija. Rad ima originalno razvijen dinamički model, eksperimentalno verifikovanu krutost i unutrašnje statičke veličine. Radom je traženo (Case Study) dejstvo vetra koje bi pri višestrukom rezonantnom naletu izazvalo gubitak dinamičke stabilnosti dizalice. Ovakvim analizama se može utvrditi realan rizik za potencijalni havarijski incident visokih objekata od ambijentalnih dejstava – meteorološki registrovanih.

Ključne reči*: opterećenje vetrom, dinamički odgovor, brodogradilišne dizalice*